ENGINEERING RESEARCH NOTE / LEO CONTROL

Feasibility Bounds for Geomagnetic Attitude Control of Very Large Flexible Space Structures

An IGRF-14 Orbit Screen, Slew Lower Bounds and Control-Structure Qualifications

Christopher I. V. Farmer

Standalone engineering article • LEO-specific feasibility study

JULY 2026

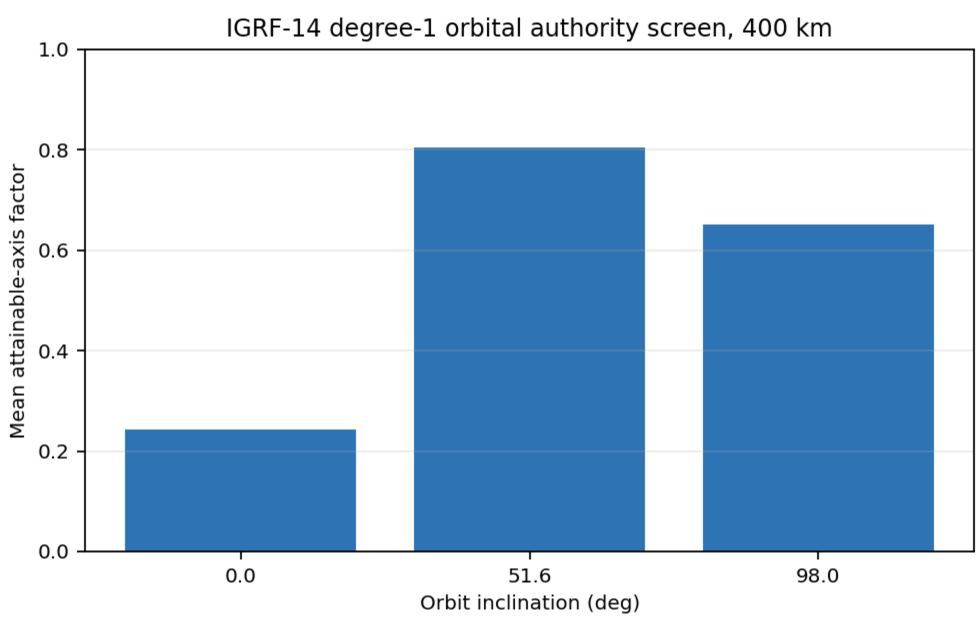

IGRF-14 screen • flexible structures • slew bounds • momentum management

Abstract

This paper derives feasibility bounds for magnetic attitude actuation of a very large flexible structure in low Earth orbit. It corrects four overclaims in an earlier version. Magnetorquers are not the only propellantless source of external torque; solar-radiation-pressure actuators, aerodynamic devices in very low orbit and electrodynamic tethers can also exchange momentum with the environment. A dipole of 10^7 A m² is an illustrative distributed-loop case, not an established hardware limit. The previously assumed orbit-averaged efficiency of 0.5-0.7 is replaced by a reproducible IGRF-14-coefficient orbit screen. Finally, low actuator bandwidth is not intrinsically safe for a flexible structure: controller harmonics, switching, field periodicity and distributed environmental loads still require a coupled control-structure model.

The reference structure is a 1,000 m by 100 m rectangular truss with mass 10^5 kg in a circular 400 km orbit. Its transverse inertia is about 8.4×10^9 kg m². A single aluminium loop around that rectangle, with 1 cm² conductor cross-section, has area 10^5 m², resistance 0.620 Ω and conductor mass about 594 kg. Currents of 1, 10 and 100 A correspond to 10^5, 10^6 and 10^7 A m², with ideal ohmic dissipation of 0.62 W, 62 W and 6.20 kW. These figures exclude switching, radiation, joints, micrometeoroid tolerance, thermal gradients and structural integration.

The orbit screen uses the official IGRF-14 2025.0 degree-1 Gauss coefficients, Earth rotation and circular orbits. At 400 km and 51.6 degrees inclination it gives 24.77-38.83 μT, mean 31.99 μT. Mean attainable-axis factors for three fixed inertial torque axes are 0.755-0.809, but instantaneous minima can be much lower. A 90-degree rest-to-rest slew in seven minutes would require about 3.0×10^5 N m. Even the optimistic maximum-field, perfect-projection lower bound requires about 6×10^9 A m²; using orbit-mean field and projection returns order 10^{10} A m². For the reference loop that implies tens to hundreds of kiloamperes and gigawatts of resistive loss. The seven-minute magnetic-only slew is therefore excluded for the reference platform.

Magnetic actuation remains valuable for detumbling, libration damping, slow biasing and momentum management when orbit geometry and the complete environmental torque budget permit. Gravity-gradient stability is conditional on principal-axis ordering and attitude, not a universally helpful dominant torque. The paper defines the simulations and experiments needed before any very-large-structure control claim can advance beyond a feasibility screen.

Keywords: magnetorquer; IGRF-14; large flexible structure; gravity gradient; attitude control; slew; control-structure interaction; momentum management.

1. Scope and contribution

The question is deliberately limited:

> *What torque and slew-time bounds follow from the geomagnetic field for a kilometre-class flexible structure in low Earth orbit, and what additional evidence is required before magnetic actuation can be called a viable controller?*

The paper does not apply outside the geomagnetic environment. A structure in cislunar or heliocentric space cannot rely on an Earth-field magnetorquer. The analysis is therefore independent of the ARGUS-PD technical series, whose candidate site is not fixed by this paper.

The principal contribution is a reproducible screen that replaces a guessed geometric "efficiency" with an orbit-dependent projection factor. It is not a controller design. It omits atmospheric and external-field disturbances, full degree-13 geomagnetism, sensor error, actuator dynamics and flexible closed-loop response.

2. Magnetic torque and instantaneous under-actuation

2.1 Torque law

A commanded magnetic dipole m in field B produces

$$\tau = m \times B, \; \| \tau \| \le m B. \tag{1}$$

For N turns, current I, loop area A and unit normal $\hat{n}$,

$$m = N I A \hat{n}. \tag{2}$$

The torque component parallel to B is identically zero. For desired torque τ_d, the minimum-norm dipole command is

$$m_{cmd} = \frac{B \times \tau_d}{B^2}, \tag{3}$$

and the realised torque is

$$\tau = \tau_d - \hat{B}\left(\tau_d \cdot \hat{B}\right). \tag{4}$$

Magnetic actuation is therefore rank two at an instant. Periodic change in the field direction can restore controllability over an orbit under appropriate orbit and inertia conditions [1-5,17,18]. Controllability does not imply high authority or arbitrary manoeuvre time; survey results for conventional small spacecraft cannot be transferred to a kilometre-class flexible structure without a new coupled model.

2.2 Fixed-axis projection factor

For a requested unit torque axis $\hat{u}$, the instantaneous fraction of the nominal $m B$ bound available about that axis is

$$\eta_u(t) = \sqrt{1 - (\hat{u} \cdot \hat{B}(t))^2}. \quad (5)$$

η_u is geometry, not conversion efficiency. It may approach zero over part of an orbit. The paper reports mean, root-mean-square and minimum values instead of assigning a universal 0.5-0.7 factor.

3. Reference structure and distributed loop

3.1 Geometry

Reference R1 is a 1,000 m by 100 m rectangular truss of mass $M = 10^5$ kg. The dimensions reconcile the inertial and loop models: the earlier paper combined a slender 1 km rod with a 1 km by 1 km current loop. That inconsistency is withdrawn.

For a uniform rectangular plate screen, the central inertias are

$$I_x = \frac{M W^2}{12} = 8.33 \times 10^7 \, kg \, m^2, \quad (6)$$

$$I_y = \frac{M L^2}{12} = 8.33 \times 10^9 \, kg \, m^2, I_z = \frac{M(L^2 + W^2)}{12} = 8.42 \times 10^9 \, kg \, m^2. \quad (7)$$

The real inertia tensor depends on distributed modules and appendages.

3.2 Loop screen

For a one-turn perimeter loop,

$$A = L W = 10^5 \, m^2, \ell = 2(L + W) = 2{,}200 \, m. \quad (8)$$

Using aluminium resistivity 2.82×10^{-8} Ωm, density 2,700 kg m⁻³ and conductor area 10^{-4} m²:

$$R = \rho \ell / a = 0.6204 \, \Omega, m_c = \rho_m \ell a = 594 \, kg. \quad (9)$$

Current	Dipole	Ideal ohmic power	Current density
1 A	10^5 A m²	0.620 W	10^4 A m⁻²
10 A	10^6 A m²	62.0 W	10^5 A m⁻²
100 A	10^7 A m²	6.20 kW	10^6 A m⁻²
100 kA	10^{10} A m²	6.20 GW	10^9 A m⁻²

The 10^7 A m² row is an aggressive illustrative calculation. It is not a flight-qualified value. A practical loop requires return paths, switches, multiple axes, joints, insulation, radiation and fault protection; its field interacts with conductive structure, instruments and plasma.

4. Geomagnetic orbit screen

4.1 Model

The reproducibility package uses the IGRF-14 2025.0 degree-1 coefficients:

$$g_1^0 = -29{,}350.0\,nT\,,\; g_1^1 = -1{,}410.3\,nT\,,\; h_1^1 = 4{,}545.5\,nT\,. \tag{10}$$

It evaluates the degree-1 scalar potential at circular-orbit positions, rotates between Earth-fixed and inertial frames, and samples one orbit. NOAA describes IGRF-14 as a degree-13 main-field model with reference radius 6,371.2 km; the present degree-1 implementation deliberately retains only the dipole terms [6-8].

This is more defensible than a single 30 μT constant but less accurate than a full IGRF-14 propagation. Mission design must use the full model and appropriate external-field and disturbance models.

4.2 Results

At 400 km:

Inclination	Field range (μT)	Mean field (μT)	Selected projection result
0 deg	24.77-25.70	25.26	ECI-Z mean 0.244
51.6 deg	24.77-38.83	31.99	fixed-axis means 0.755-0.809
98 deg	24.77-49.54	38.07	axis-dependent means 0.639-0.995

At 51.6 degrees the RMS factors for the ECI-X, ECI-Y and ECI-Z axes are 0.822, 0.783 and 0.844, respectively. The minima are 0.569, 0.400 and 0.116. A mean factor therefore cannot guarantee continuous authority.

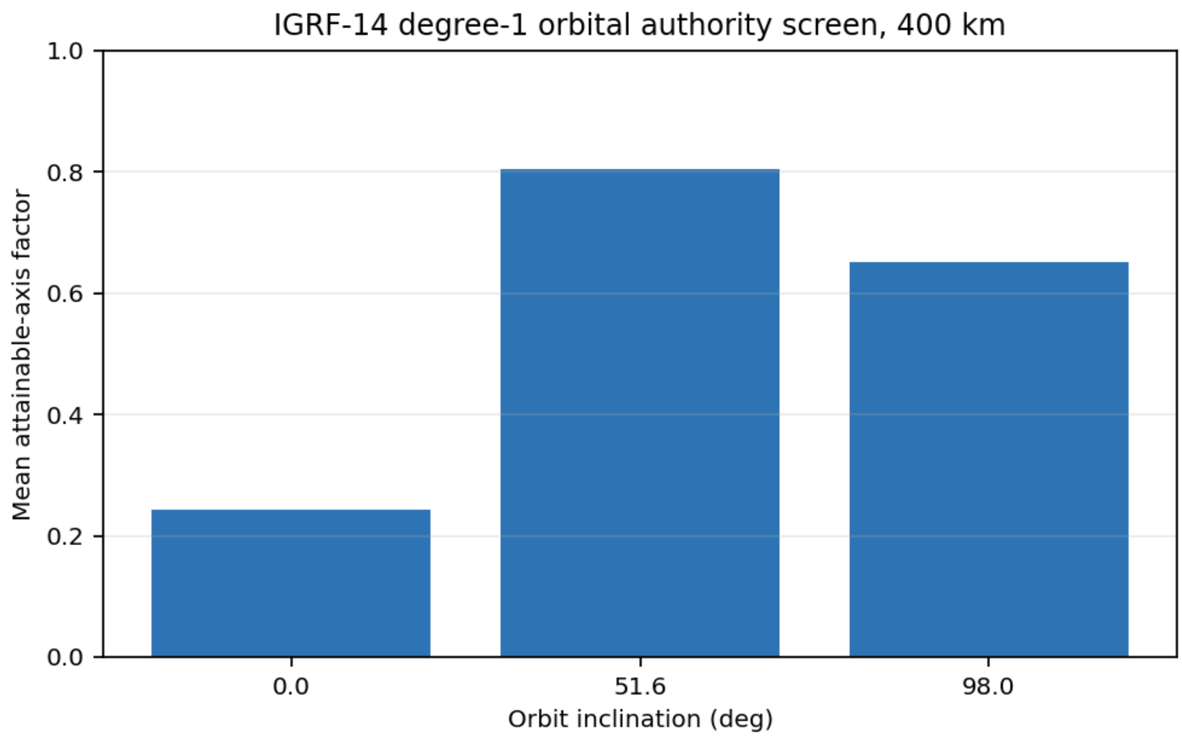

Mean fixed-axis magnetic authority for the ECI-Z axis in the reproducible IGRF-14 degree-1 screen.

The equatorial case demonstrates the geometric weakness that a universal factor obscures: torque about an axis near the persistent field direction is poor even if torque about orthogonal axes is strong.

5. Slew lower bounds

5.1 Rest-to-rest bound

For a rigid-body eigenaxis rotation through angle $\Delta\theta$, with bounded constant torque τ, the ideal bang-bang lower bound is

$$t_{min} = 2\sqrt{\frac{I\,\Delta\theta}{\tau}}. \tag{11}$$

If a constant screening factor η is temporarily used,

$$\tau_{eff} = \eta\, m\, B, t_{min} = 2\sqrt{\frac{I\,\Delta\theta}{\eta\, m\, B}}. \tag{12}$$

For a required time,

$$m_{req} = \frac{4 I \Delta\theta}{\eta B t^2}. \tag{13}$$

The earlier version incorrectly stated that required dipole increased as $1/\sqrt{\eta}$. Equation (13) shows that it increases as $1/\eta$; slew time increases as $1/\sqrt{\eta}$.

5.2 Seven-minute question

Using $I = 8.42 \times 10^9$ kg m², $\Delta\theta = \pi/2$ and $t = 420$ s:

$$\tau_{req} = \frac{4 I \Delta\theta}{t^2} \approx 3.0 \times 10^5\, N\, m. \tag{14}$$

With the most optimistic field observed in the 400 km screen, $B = 49.54\,\mu$T, and perfect projection, the absolute lower bound is

$$m_{req} > 6.0 \times 10^9\, A\, m^2. \tag{15}$$

At 51.6 degrees, using the 31.99 μT mean field and a representative mean projection near 0.8 gives

$$m_{req} \approx 1.2 \times 10^{10}\, A\, m^2. \tag{16}$$

These are optimistic rigid-body values. They exclude structural input shaping, actuator current dynamics, saturation, disturbance rejection and intervals of low authority. In the reference loop, 10^{10} A m² requires 100 kA and about 6.2 GW ideal ohmic loss. The seven-minute magnetic-only slew is excluded by orders of magnitude.

5.3 Slow-slew table

Using the 51.6-degree mean field only and perfect projection as a lower bound:

Dipole	Nominal torque	90-degree rigid lower bound
10^5 A m²	3.20 N m	about 36 h
10^6 A m²	32.0 N m	about 11.3 h
10^7 A m²	320 N m	about 3.6 h

Orbit projection, flexible-body constraints and controller limits increase these values. “Hours to days” is a defensible research envelope for R1; “seven minutes” is not.

6. Gravity-gradient torque

For circular orbit radius r, nadir unit vector $\hat{n}$ and inertia tensor I,

$$\tau_{gg} = 3\frac{\mu_E}{r^3}(\hat{n} \times I\hat{n}). \tag{17}$$

For a principal-axis displacement ϕ, a representative magnitude is

$$\tau_{gg} = \frac{3}{2}n^2 \Delta I \sin 2\phi, \tag{18}$$

where n is mean motion. At 400 km, $n \approx 1.133 \times 10^{-3}$ rad s^{-1}. With $\Delta I \approx 8.25 \times 10^9$ kg m², the peak screen is about 1.59×10^4 N m.

That value exceeds the 10^7 A m² mean magnetic torque by a factor of roughly 50. It does **not** follow that gravity gradient is always helpful. Passive stability requires a suitable ordering of principal inertias and alignment relative to the local vertical and orbit normal [9-12]. Appendages, fuel motion, deployed cables, thermal distortion and flexibility can change the inertia tensor and introduce unstable or weakly damped modes.

For the ideal rectangular reference, the minimum-inertia axis can align with the local vertical and the maximum-inertia axis with the orbit normal, creating a gravity-gradient equilibrium. The equilibrium is conservative and requires damping. Magnetic actuation may be suitable near it, but it cannot generally hold an arbitrary attitude against the peak gravity-gradient torque.

7. Momentum management and other external torques

Internal wheels or control-moment gyros redistribute angular momentum but saturate under secular environmental torque. An external torque is needed to change the spacecraft-environment angular-momentum balance.

Magnetorquers are a mature propellantless method in LEO, but not the only possibility:

- **solar-radiation-pressure devices** can generate control torque through movable reflectors, centre-of-pressure offset or optical-property control;
- **aerodynamic control surfaces** can create torque in sufficiently low orbit, with drag and atmospheric variability;
- **electrodynamic tethers** exchange momentum and energy with the ionospheric plasma and geomagnetic field;
- **gravity-gradient shaping** provides conservative environmental torque and can support equilibrium or manoeuvre strategies; and

- **differential reflectivity or drag** can provide slow environmental control in suitable regimes.

Each alternative has orbit and configuration limits. A systems comparison should optimise a hybrid external-torque portfolio rather than assuming magnetic exclusivity.

8. Flexible-structure dynamics

8.1 Modal uncertainty

For a uniform Euler-Bernoulli beam, a representative bending frequency is

$$\omega_j = \frac{\lambda_j^2}{L^2}\sqrt{\frac{EI_b}{\mu}}, \tag{19}$$

where EI_b is bending stiffness, μ linear density and λ_j depends on boundary conditions [13-16]. R1 cannot be assigned a credible first mode without its truss geometry, joints, tension state, appendages and distributed masses. A single illustrative 10^{-2} Hz value is therefore not a controlled property.

8.2 Why low bandwidth is not automatically safe

A slowly varying commanded torque may reduce direct excitation above the first mode, but four qualifications prevent a categorical “spectral separation” claim:

1. the geomagnetic field and controller are periodic and contain harmonics;
2. switching and saturation introduce broadband content;
3. distributed magnetic forces may not be equivalent to a pure rigid-body torque;
4. thermal snap, gravity-gradient variation, aerodynamic load and actuator faults can excite low modes independently.

The correct design requirement is a coupled model with modal participation, actuator placement, sensor dynamics, spillover analysis and robust stability margin. Input shaping and low-pass command design may help after modal identification; slowness alone is not proof.

8.3 Distributed loads

A kilometre-class structure experiences:

- gravity-gradient variation along its length;
- nonuniform geomagnetic field and current-path forces;
- thermal gradients and moving shadow boundaries;
- aerodynamic and charged-particle effects in LEO;
- solar-radiation-pressure distribution; and

- local failures, deployment tolerances and joint nonlinearities.

Attitude and structure must therefore be simulated together.

9. Feasibility envelope

Task	Magnetic contribution	Evidence level
coarse detumble	plausible over multiple orbits	controller and flexible simulation required
libration damping near a valid gravity-gradient equilibrium	supported by small-spacecraft theory; scale unvalidated	representative distributed-actuator test
momentum unloading	plausible and classical in LEO	complete disturbance and authority budget
slow bias or repointing	hours-to-days screen for R1	orbit-specific nonlinear simulation
seven-minute 90-degree slew	excluded for R1	lower bound already fails
arbitrary attitude against peak gravity gradient	generally not magnetic-only	hybrid actuator or different equilibrium
cislunar/heliocentric control	geomagnetic method inapplicable	other actuators required

10. Verification programme

1. **Full-field orbit analysis:** propagate IGRF-14 degree 13, Earth rotation, selected orbit, secular variation and appropriate external-field models.
2. **Inertia and flexible model:** identify the deployed inertia tensor, modes, damping and thermal distortion.
3. **Distributed-loop prototype:** measure resistance, inductance, electromagnetic compatibility, thermal rejection and fault isolation.
4. **Controllability and authority map:** compute time-varying controllability Gramians and axis-specific dead zones.
5. **Control-structure analysis:** include actuator/sensor dynamics, saturation, harmonics, spillover and robust margins.
6. **Environmental torque budget:** include gravity gradient, drag, radiation pressure, tethers if used, residual magnetic moment and appendage motion.
7. **Hardware-in-the-loop demonstration:** verify acquisition, damping, momentum management and safe-mode behaviour with scaled flexible dynamics.

Failure to obtain adequate authority or robust stability leads to a hybrid actuator or a different orbit; it is not repaired by increasing an assumed efficiency factor.

11. Conclusion

Magnetic actuation of a very large LEO structure is physically meaningful but strongly task-limited. A reconciled 1 km by 100 m reference geometry makes a 10^7 A m² distributed loop arithmetically expressible at kilowatt ohmic power, although integration and qualification remain open. IGRF-14 degree-1 orbit propagation shows why one field magnitude and one efficiency factor are inadequate: field and attainable-axis projection vary with inclination, axis and orbital phase.

The seven-minute slew result is a robust negative finding. It requires about 3×10^5 N m and at least several 10^9 A m², reaching order 10^{10} A m² under representative mean field and projection. The reference loop would require gigawatts of dissipation. Magnetic-only operation is instead a candidate for slow damping, biasing and momentum management near a suitable environmental equilibrium.

Gravity-gradient torque is conditional, other propellantless environmental actuators exist, and flexible-body safety requires coupled analysis. Those qualifications narrow the conclusion but strengthen it: magnetic control may be useful precisely where its orbit-dependent authority is matched to a slow, measured and robustly controlled task.

Declarations

Funding. No external funding is declared.

Competing interests. The author declares no competing financial interest.

Data and code availability. The degree-1 IGRF-14 orbit screen, loop calculator, unit tests, machine-readable tables and figure script accompany the paper. The code states its low-degree limitation.

References

1. Stickler, A. C. & Alfriend, K. T. Elementary magnetic attitude control system. *Journal of Spacecraft and Rockets* 13, 282-287 (1976). https://doi.org/10.2514/3.57089.
2. Wisniewski, R. & Blanke, M. Fully magnetic attitude control for spacecraft subject to gravity gradient. *Automatica* 35, 1201-1214 (1999). https://doi.org/10.1016/S0005-1098(99)00021-7.
3. Psiaki, M. L. Magnetic torquer attitude control via asymptotic periodic linear quadratic regulation. *Journal of Guidance, Control, and Dynamics* 24, 386-394 (2001). https://doi.org/10.2514/2.4723.
4. Lovera, M. & Astolfi, A. Spacecraft attitude control using magnetic actuators. *Automatica* 40, 1405-1414 (2004). https://doi.org/10.1016/j.automatica.2004.02.022.
5. Bhat, S. P. Controllability of nonlinear time-varying systems: applications to spacecraft attitude control using magnetic actuation. *IEEE Transactions on Automatic Control* 50, 1725-1735 (2005). https://doi.org/10.1109/TAC.2005.858686.
6. NOAA National Centers for Environmental Information. International Geomagnetic Reference Field: 14th generation release and coefficients (accessed 23 July 2026). https://www.ncei.noaa.gov/products/international-geomagnetic-reference-field.
7. British Geological Survey. International Geomagnetic Reference Field (IGRF), 14th-generation calculator (accessed 23 July 2026). https://geomag.bgs.ac.uk/data_service/models_compass/igrf_calc.html.
8. Beggan, C. D., Thébault, E. et al. International geomagnetic reference field: the fourteenth generation. *Earth, Planets and Space* 78, 127 (2026). https://doi.org/10.1186/s40623-025-02360-0.
9. Wertz, J. R. (ed.). *Spacecraft Attitude Determination and Control*. Reidel (1978).
10. Hughes, P. C. *Spacecraft Attitude Dynamics*. Wiley (1986).
11. Sidi, M. J. *Spacecraft Dynamics and Control*. Cambridge University Press (1997).
12. Markley, F. L. & Crassidis, J. L. *Fundamentals of Spacecraft Attitude Determination and Control*. Springer (2014). https://doi.org/10.1007/978-1-4939-0802-8.
13. Balas, M. J. Trends in large space structure control theory. *IEEE Transactions on Automatic Control* 27, 522-535 (1982). https://doi.org/10.1109/TAC.1982.1102953.
14. Meirovitch, L. *Dynamics and Control of Structures*. Wiley (1990).
15. Junkins, J. L. & Kim, Y. *Introduction to Dynamics and Control of Flexible Structures*. AIAA (1993). https://doi.org/10.2514/4.862076.
16. Blevins, R. D. *Formulas for Natural Frequency and Mode Shape*. Van Nostrand Reinhold (1979).
17. Ovchinnikov, M. Y. & Roldugin, D. S. A survey on active magnetic attitude-control algorithms for small satellites. *Progress in Aerospace Sciences* 109, 100546 (2019). https://doi.org/10.1016/j.paerosci.2019.05.006.
18. Silani, E. & Lovera, M. Magnetic spacecraft attitude control: a survey and some new results. *Control Engineering Practice* 13, 357-371 (2005). https://doi.org/10.1016/j.conengprac.2003.12.017.